

Imaging topological defects in a non-collinear antiferromagnet

Aurore Finco

Laboratoire Charles Coulomb
Team Solid-State Quantum Technologies (S2QT)

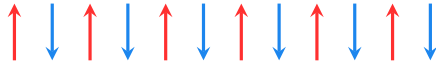
CNRS and Université de Montpellier, Montpellier, France



MMM 2022, Minneapolis

slides available at <https://magimag.eu>

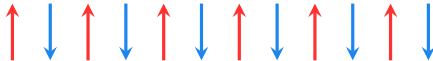
Imaging antiferromagnets



“They are extremely interesting from the theoretical viewpoint, but do not seem to have any applications.”

Louis Néel, *Nobel lecture* (1970)

Imaging antiferromagnets



“They are extremely interesting from the theoretical viewpoint, but do not seem to have any applications.”

Louis Néel, *Nobel lecture* (1970)

- Antiferromagnetic spintronics
 - V. Baltz *et al.* *Rev. Mod. Phys.* 90 (2018)
 - T. Jungwirth *et al.* *Nat. Nano.* 11 (2016), 231
- Multiferroics are mostly antiferromagnetic
 - M. Fiebig *et al.* *Nat. Rev. Mater.* 1 (2016), 1

Imaging antiferromagnets



"They are extremely interesting from the theoretical viewpoint, but do not seem to have any applications."

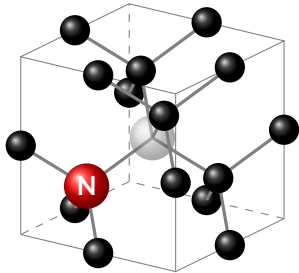
Louis Néel, *Nobel lecture* (1970)

- Antiferromagnetic spintronics
 - V. Baltz *et al.* *Rev. Mod. Phys.* 90 (2018)
 - T. Jungwirth *et al.* *Nat. Nano.* 11 (2016), 231
- Multiferroics are mostly antiferromagnetic
 - M. Fiebig *et al.* *Nat. Rev. Mater.* 1 (2016), 1

Imaging antiferromagnets remains complicated!

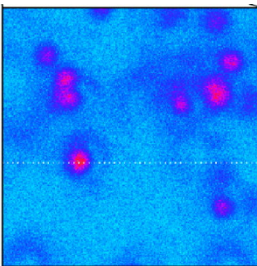
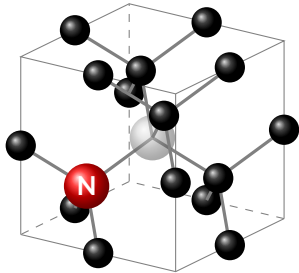
■ S.-W. Cheong *et al.* *npj Quantum Materials* 5 (2020)

Our magnetic field sensor: the NV center in diamond



Nitrogen-Vacancy defect

Our magnetic field sensor: the NV center in diamond



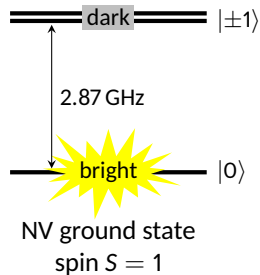
Nitrogen-Vacancy defect

- Photostable defect
- Spin $S=1$
- Individual defects can be isolated/implanted
- Ambient conditions

A. Gruber et al. *Science* 276 (1997), 2012

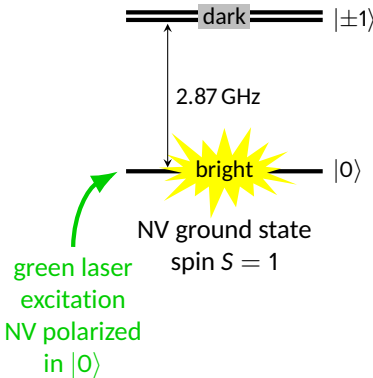
Principle of the magnetic field measurement

Spin-dependent
fluorescence

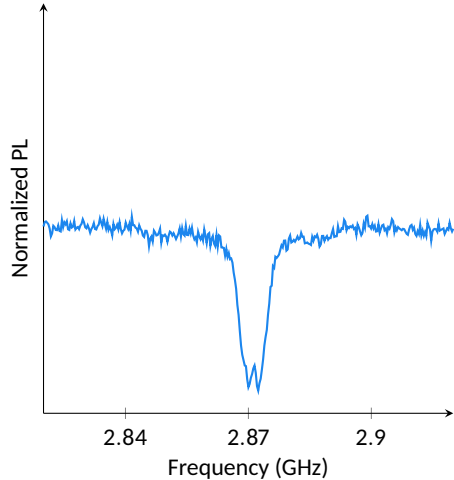
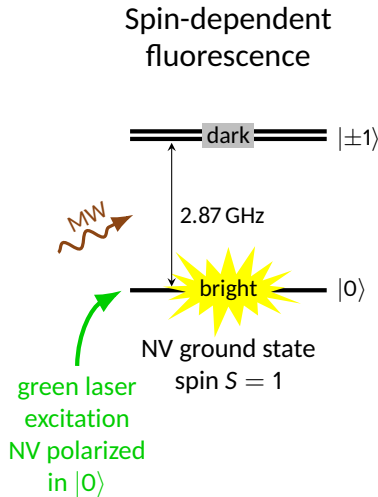


Principle of the magnetic field measurement

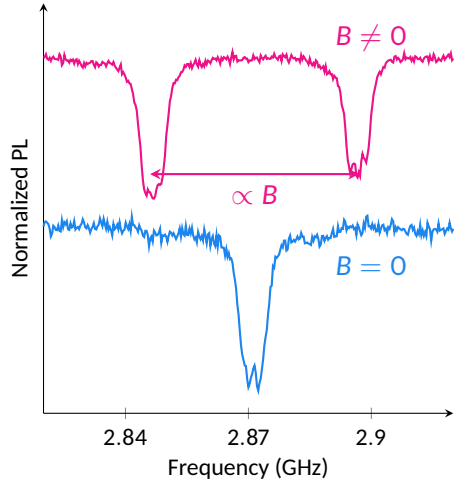
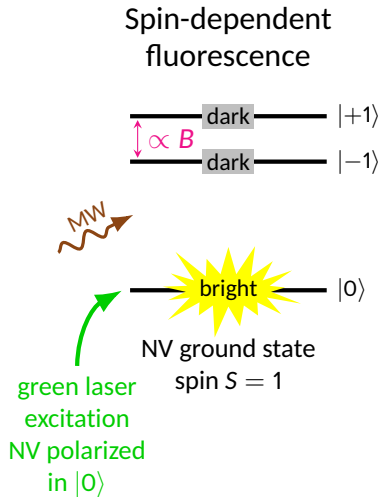
Spin-dependent
fluorescence



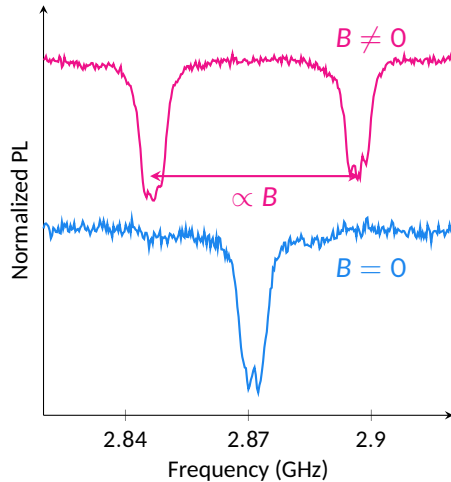
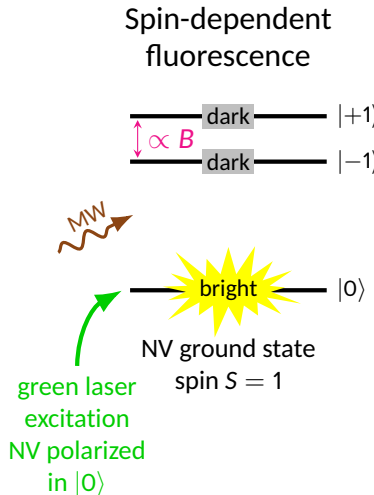
Principle of the magnetic field measurement



Principle of the magnetic field measurement



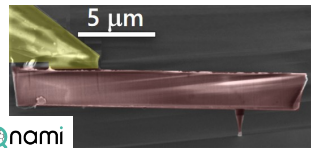
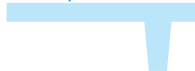
Principle of the magnetic field measurement



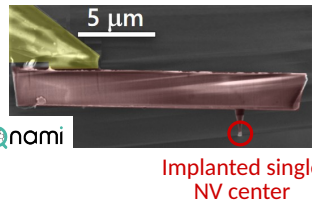
Sensibility: a few $\mu\text{T}/\sqrt{\text{Hz}}$

The scanning NV microscope setup

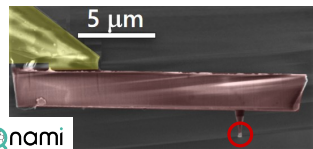
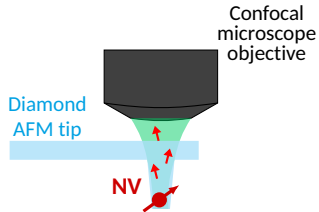
Diamond
AFM tip



The scanning NV microscope setup

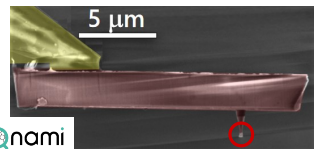
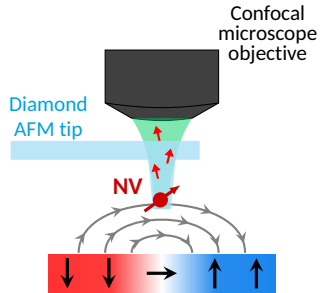


The scanning NV microscope setup



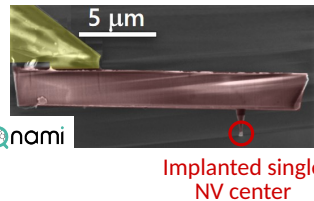
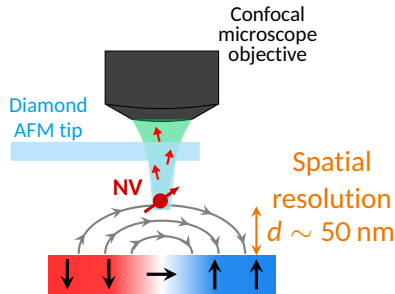
Implanted single
NV center

The scanning NV microscope setup



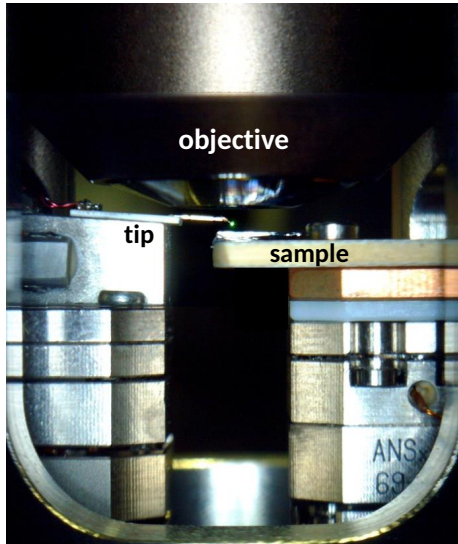
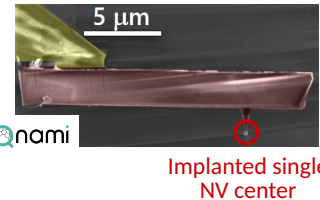
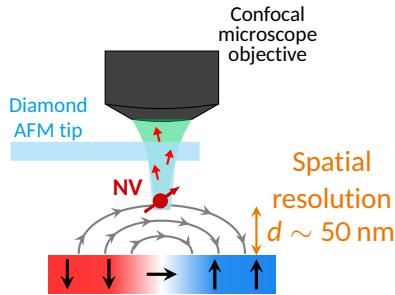
Implanted single
NV center

The scanning NV microscope setup



P. Maletinsky et al. *Nat. Nano.* 7 (2012), 320

The scanning NV microscope setup



Application to nanoscale magnetic texture imaging

Quantitative

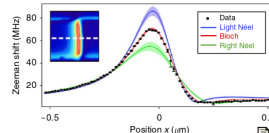
Non-perturbative

Highly sensitive

Application to nanoscale magnetic texture imaging

Determination of domain wall chirality

Quantitative



J.-P. Tetienne et al. *Nat Commun.* 6 (2015), 6733

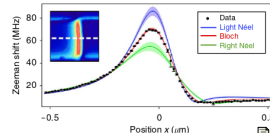
Non-perturbative

Highly sensitive

Application to nanoscale magnetic texture imaging

Quantitative

Determination of domain wall chirality

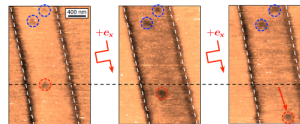


J.-P. Tetienne et al. *Nat Commun.* 6 (2015), 6733

Non-perturbative

Highly sensitive

Imaging of current-induced skyrmion movement

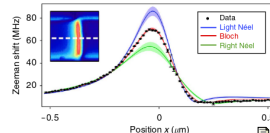


W. Akhtar et al. *Phys. Rev. Appl.* 11 (2019), 034066

Application to nanoscale magnetic texture imaging

Quantitative

Determination of domain wall chirality

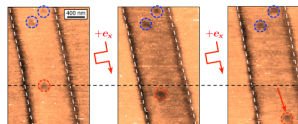


J.-P. Tetienne et al. *Nat Commun.* 6 (2015), 6733

Non-perturbative

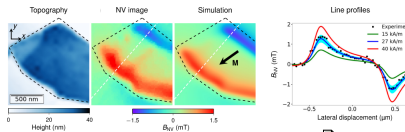
Highly sensitive

Imaging of current-induced skyrmion movement



W. Akhtar et al. *Phys. Rev. Appl.* 11 (2019), 034066

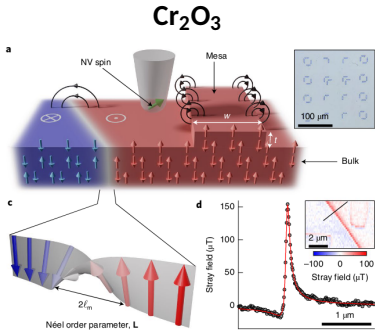
Quantitative characterization of 2D ferromagnets



F. Fabre et al. *Phys. Rev. Mat.* 5 (2021), 034008

What about antiferromagnets?

Small stray field measurements

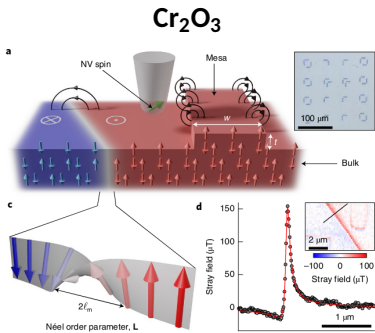


■ N. Hedrich et al. *Nat. Phys.* 17 (2021), 574

See talk by K. Wagner SC-O5/CA-04

What about antiferromagnets?

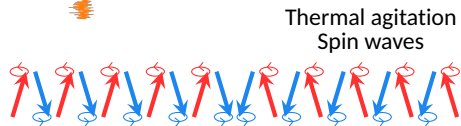
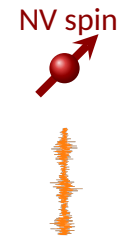
Small stray field measurements



■ N. Hedrich et al. *Nat. Phys.* 17 (2021), 574

See talk by K. Wagner SC-O5/CA-04

Magnetic noise detection

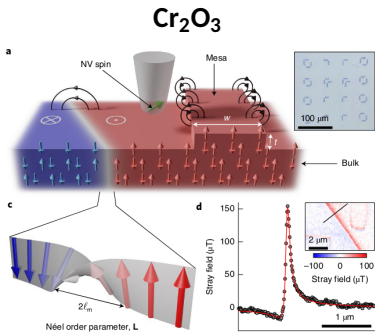


■ B. Flebus et al. *Phys. Rev. B* 98 (2018), 180409

■ A. Finco et al. *Nat. Commun.* 12 (2021), 767

What about antiferromagnets?

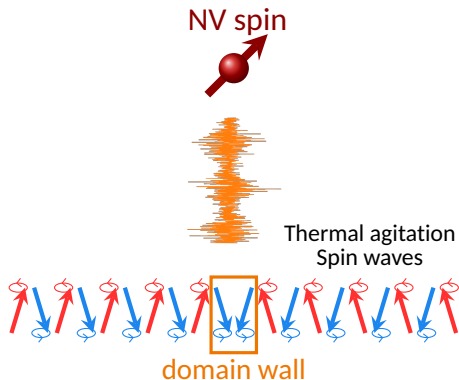
Small stray field measurements



N. Hedrich et al. *Nat. Phys.* 17 (2021), 574

See talk by K. Wagner SC-O5/CA-04

Magnetic noise detection

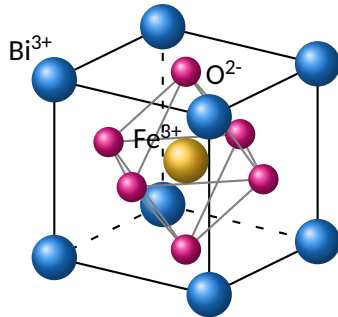


B. Flebus et al. *Phys. Rev. B* 98 (2018), 180409

A. Finco et al. *Nat. Commun.* 12 (2021), 767

Bismuth ferrite, a room-temperature multiferroic

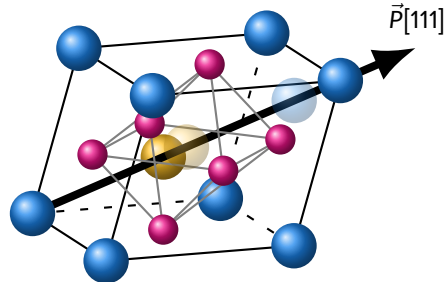
Electric polarization



Paraelectric phase ($T > 1100$ K)

Bismuth ferrite, a room-temperature multiferroic

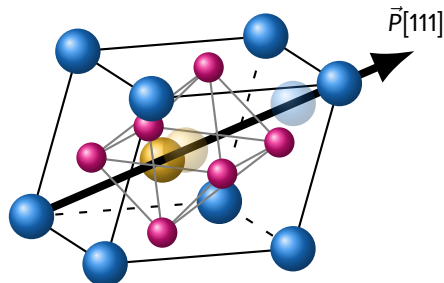
Electric polarization



Ferroelectric phase ($T < 1100$ K)

Bismuth ferrite, a room-temperature multiferroic

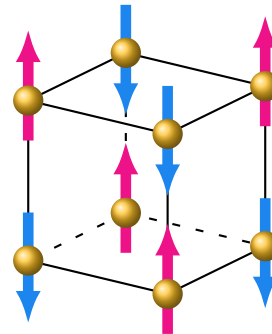
Electric polarization



Ferroelectric phase ($T < 1100$ K)

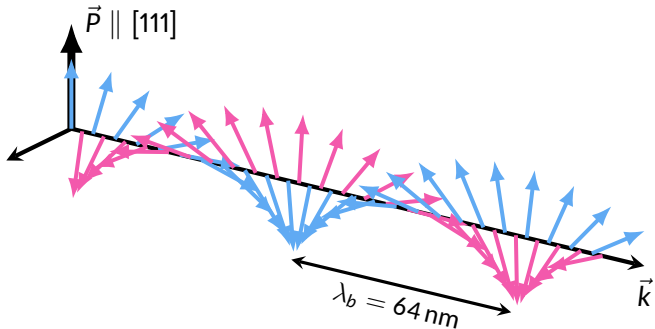
G. Catalan et al. *Adv. Mater.* 21 (2009), 2463–2485

Magnetism



G-type antiferromagnetic
phase ($T_N = 643$ K)

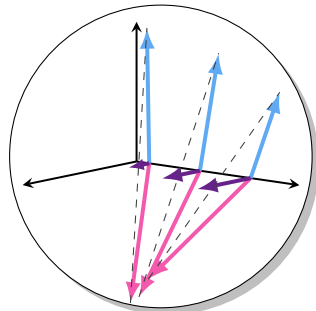
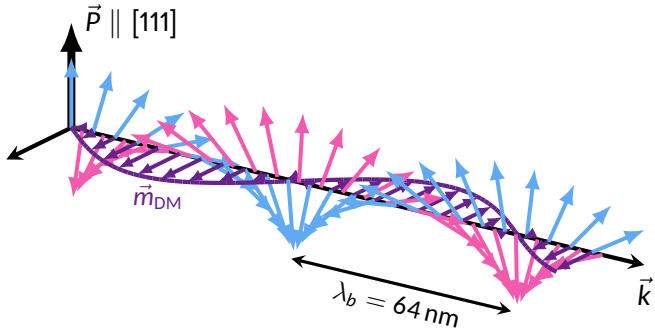
The effects of magnetoelectric coupling in BiFeO₃



Fully compensated cycloid

→ **No stray field!**

The effects of magnetoelectric coupling in BiFeO₃

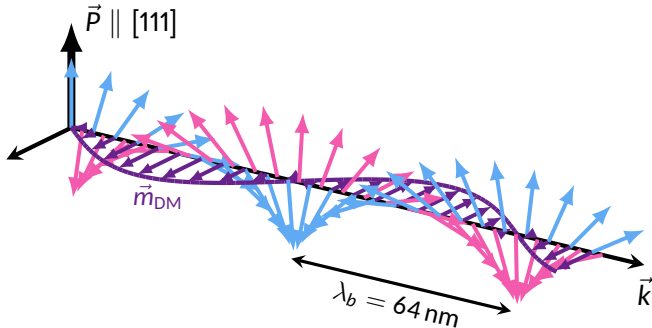


Spin density wave

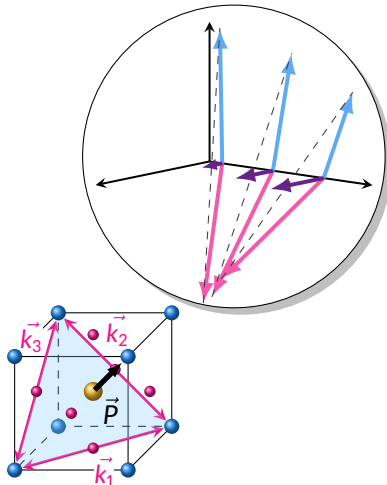
Weak uncompensated moment

→ Small stray field

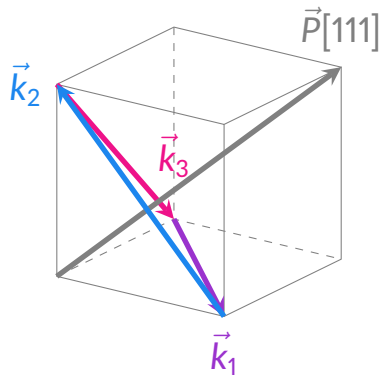
The effects of magnetoelectric coupling in BiFeO₃



Spin density wave
Weak uncompensated moment
→ Small stray field



The bulk-like cycloid

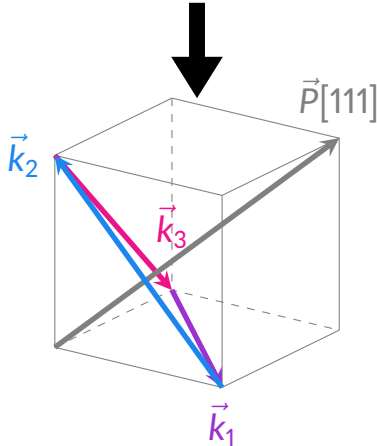


$$\vec{k}_1 \parallel [\bar{1}\bar{1}0]$$

$$\vec{k}_2 \parallel [\bar{1}01]$$

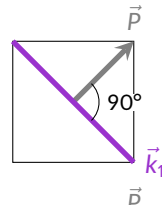
$$\vec{k}_3 \parallel [01\bar{1}]$$

The bulk-like cycloid

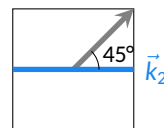


$$\begin{aligned}\vec{k}_1 &\parallel [1\bar{1}0] \\ \vec{k}_2 &\parallel [\bar{1}01] \\ \vec{k}_3 &\parallel [01\bar{1}]\end{aligned}$$

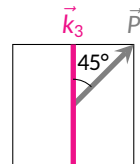
Top view



$$\begin{aligned}\lambda_{IP} &= \lambda_b \\ 64 \text{ nm}\end{aligned}$$



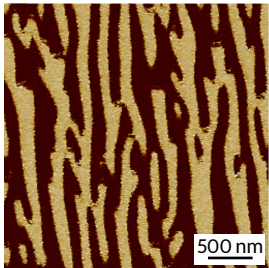
$$\begin{aligned}\lambda_{IP} &= \sqrt{2}\lambda_b \\ 90 \text{ nm}\end{aligned}$$



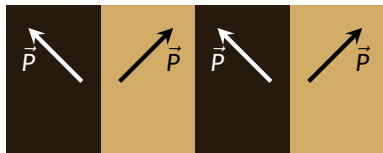
$$\begin{aligned}\lambda_{IP} &= \sqrt{2}\lambda_b \\ 90 \text{ nm}\end{aligned}$$

The cycloid in a low strained BiFeO₃ thin film

Collaborations: UMR CNRS/Thales, Palaiseau (V. Garcia, S. Fusil)

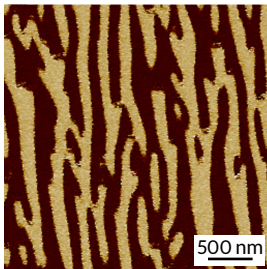


PFM image
ferroelectric domains

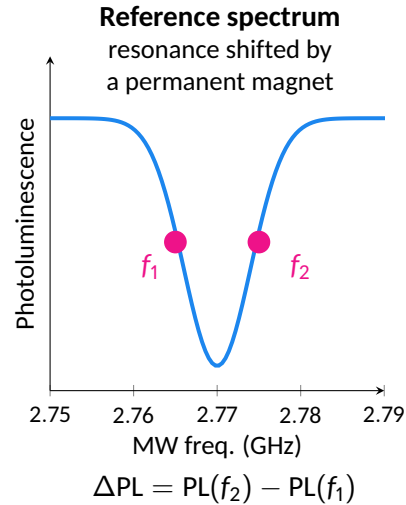
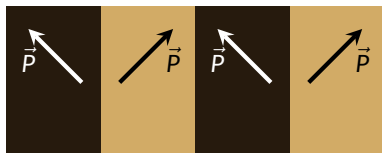


The cycloid in a low strained BiFeO₃ thin film

Collaborations: UMR CNRS/Thales, Palaiseau (V. Garcia, S. Fusil)

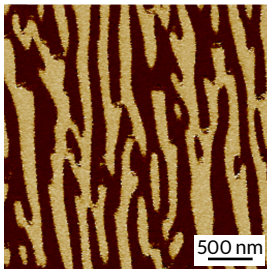


PFM image
ferroelectric domains

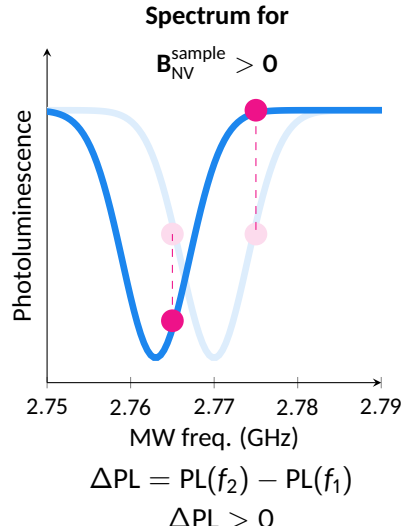
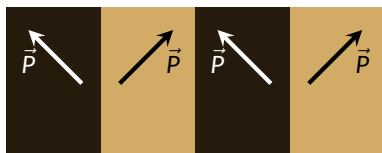


The cycloid in a low strained BiFeO₃ thin film

Collaborations: UMR CNRS/Thales, Palaiseau (V. Garcia, S. Fusil)

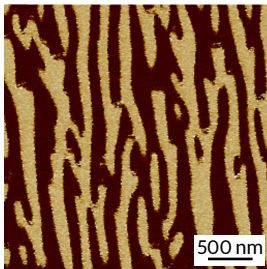


PFM image
ferroelectric domains

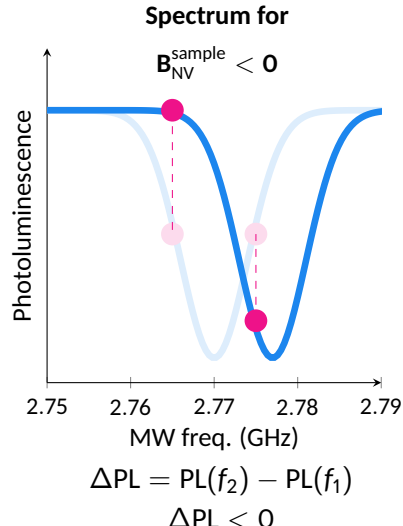
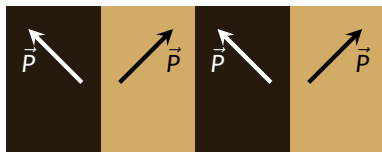


The cycloid in a low strained BiFeO₃ thin film

Collaborations: UMR CNRS/Thales, Palaiseau (V. Garcia, S. Fusil)

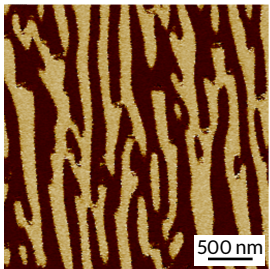


PFM image
ferroelectric domains

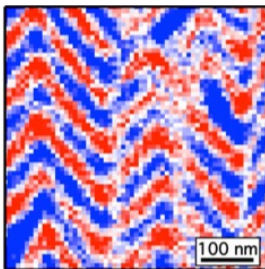


The cycloid in a low strained BiFeO₃ thin film

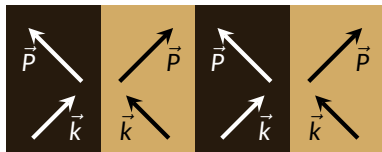
Collaborations: UMR CNRS/Thales, Palaiseau (V. Garcia, S. Fusil)



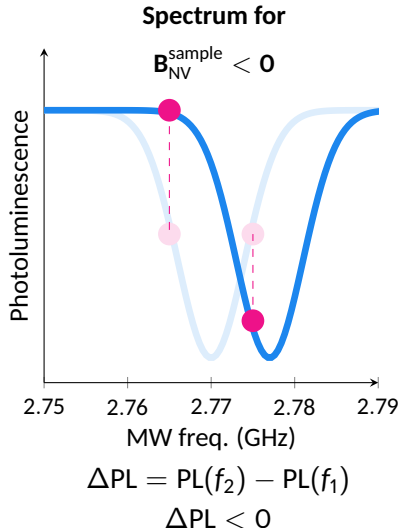
PFM image
ferroelectric domains



NV image
cycloid

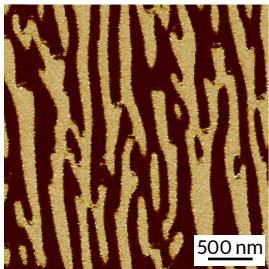


\vec{k}_1 wavevector

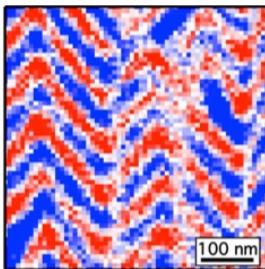


The cycloid in a low strained BiFeO₃ thin film

Collaborations: UMR CNRS/Thales, Palaiseau (V. Garcia, S. Fusil)

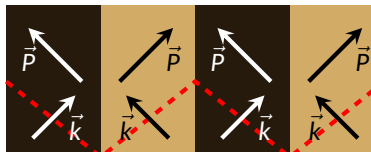


PFM image
ferroelectric domains

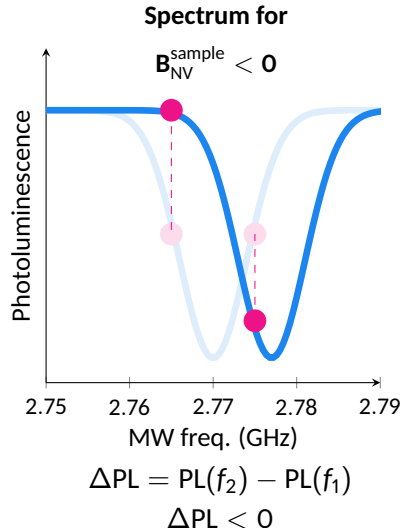


NV image
cycloid

iso-B
signal
norm.
1
0
-1

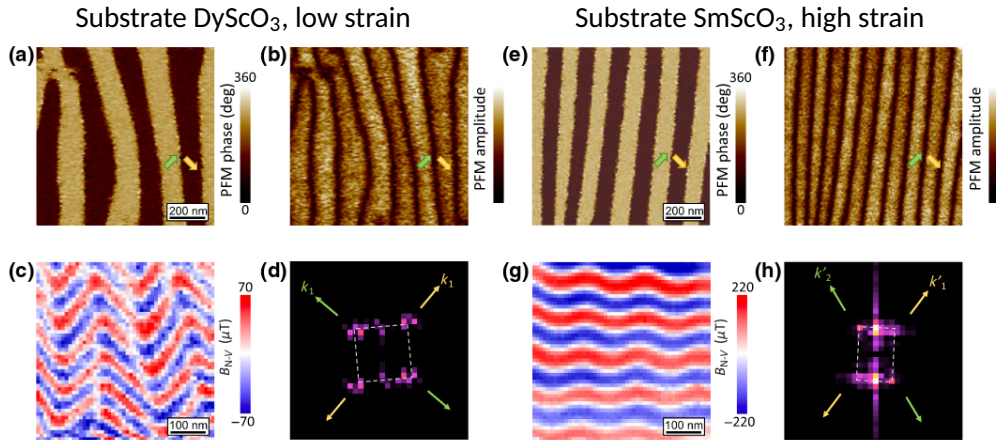


\vec{k}_1 wavevector



Stabilizing an exotic cycloid type with strain

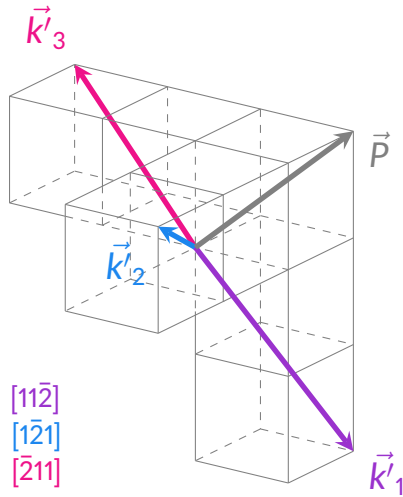
Collaborations: UMR CNRS/Thales, Palaiseau (V. Garcia, S. Fusil), Qnami, Basel (H. Zhong)



H. Zhong et al. *Phys. Rev. Appl.* 17 (2022), 044051

A. Haykal et al. *Nat. Commun.* 11 (2020), 1704

The type II cycloid

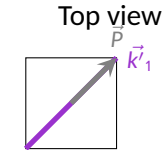
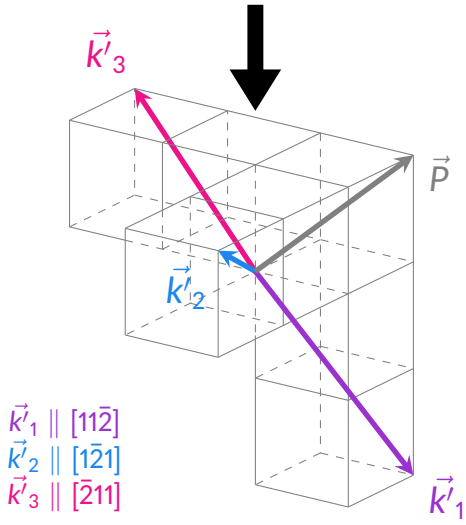


$$\vec{k}'_1 \parallel [11\bar{2}]$$

$$\vec{k}'_2 \parallel [1\bar{2}1]$$

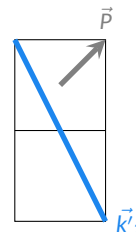
$$\vec{k}'_3 \parallel [\bar{2}11]$$

The type II cycloid



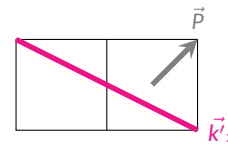
$$\lambda_{IP} = \sqrt{3}\lambda_b$$

111 nm



$$\lambda_{IP} = \sqrt{\frac{6}{5}}\lambda_b$$

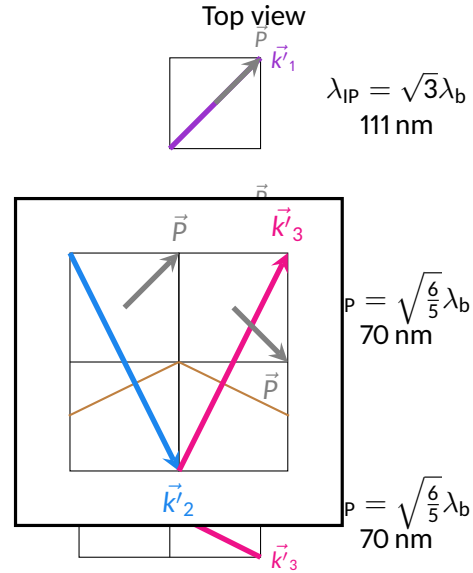
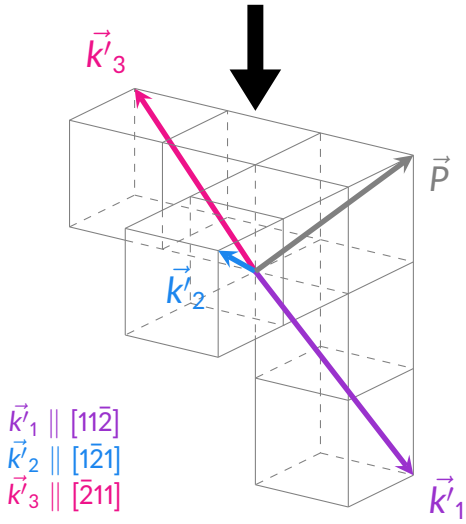
70 nm



$$\lambda_{IP} = \sqrt{\frac{6}{5}}\lambda_b$$

70 nm

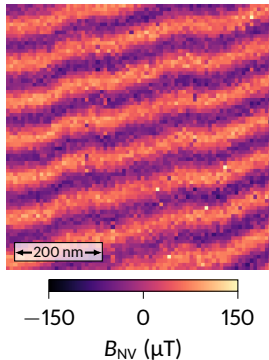
The type II cycloid



Quantitative analysis of the cycloid in bulk single crystal

Collaborations: UMR CNRS/Thales, Palaiseau (V. Garcia, S. Fusil)

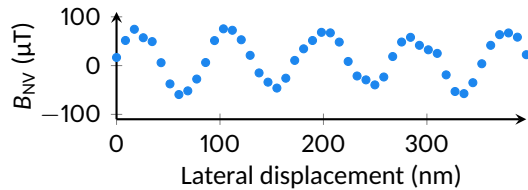
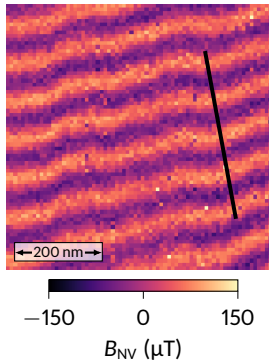
CEA SPEC, Gif-sur-Yvette (J.-Y. Chauleau, M. Viret)



Quantitative analysis of the cycloid in bulk single crystal

Collaborations: UMR CNRS/Thales, Palaiseau (V. Garcia, S. Fusil)

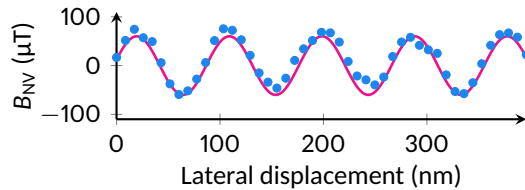
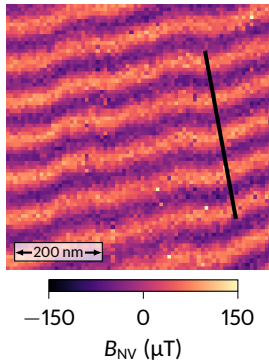
CEA SPEC, Gif-sur-Yvette (J.-Y. Chauleau, M. Viret)



Quantitative analysis of the cycloid in bulk single crystal

Collaborations: UMR CNRS/Thales, Palaiseau (V. Garcia, S. Fusil)

CEA SPEC, Gif-sur-Yvette (J.-Y. Chauleau, M. Viret)

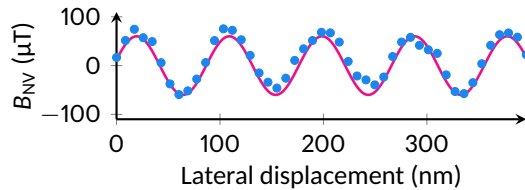
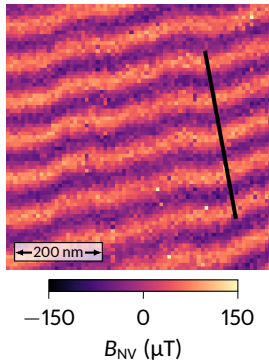


$$\begin{cases} B_x = 0 \\ B_y = -\frac{A}{\sqrt{2}} (\text{Re}\{S\} - \text{Im}\{S\}) \\ B_z = \sqrt{2} A \text{Re}\{S\} \end{cases} \quad \text{with} \quad \begin{cases} A = \frac{\mu_0 m_{\text{DM}}}{\sqrt{3} a^3} \sinh\left(\frac{ka}{2\sqrt{2}}\right) \\ S = e^{-kz/\sqrt{2}} e^{ik(y-z)/\sqrt{2}} \frac{1 - e^{-kt(1+i)/\sqrt{2}}}{1 - e^{-ka(1+i)/\sqrt{2}}} \end{cases}$$

Quantitative analysis of the cycloid in bulk single crystal

Collaborations: UMR CNRS/Thales, Palaiseau (V. Garcia, S. Fusil)

CEA SPEC, Gif-sur-Yvette (J.-Y. Chauleau, M. Viret)



$$m_{\text{DM}} = 0.09 \pm 0.03 \mu_{\text{B}}$$

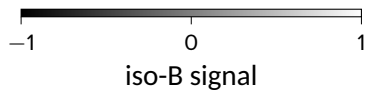
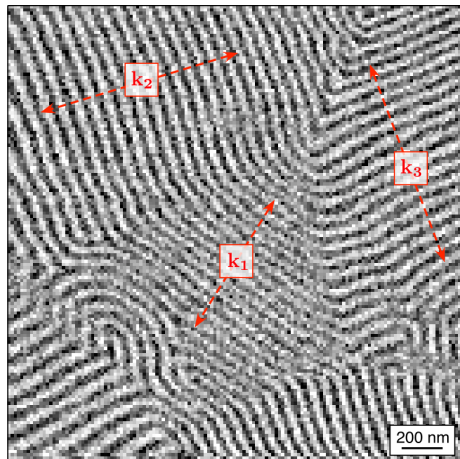
M. Ramazanoglu et al. *Phys. Rev. Lett.* 107 (2011), 207206

$$\begin{cases} B_x = 0 \\ B_y = -\frac{A}{\sqrt{2}} (\text{Re}\{S\} - \text{Im}\{S\}) \\ B_z = \sqrt{2} A \text{Re}\{S\} \end{cases}$$

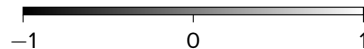
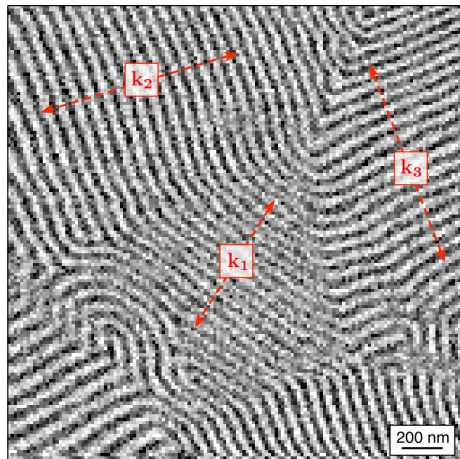
with

$$\begin{cases} A = \frac{\mu_0 m_{\text{DM}}}{\sqrt{3} a^3} \sinh\left(\frac{ka}{2\sqrt{2}}\right) \\ S = e^{-kz/\sqrt{2}} e^{ik(y-z)/\sqrt{2}} \frac{1 - e^{-kt(1+i)/\sqrt{2}}}{1 - e^{-ka(1+i)/\sqrt{2}}} \end{cases}$$

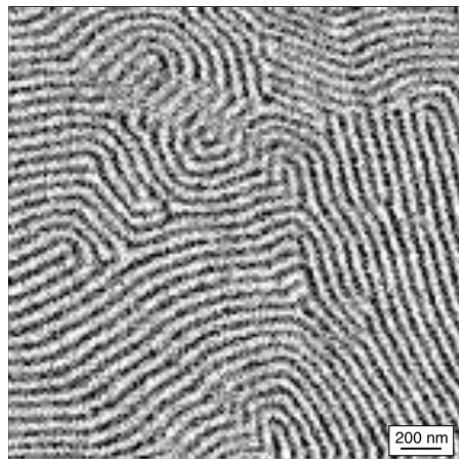
Rotation of the cycloid propagation direction measured in real space...



Rotation of the cycloid propagation direction measured in real space...



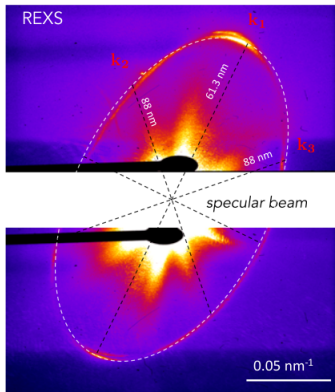
iso-B signal



iso-B signal

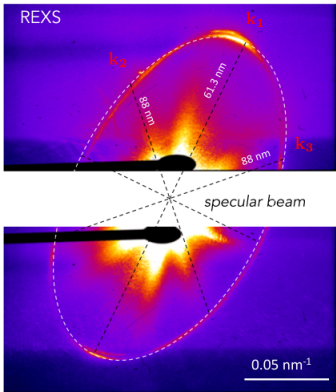
... and in reciprocal space

Resonant X-ray scattering

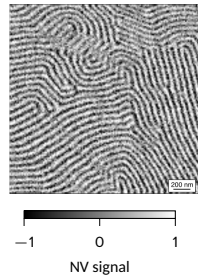
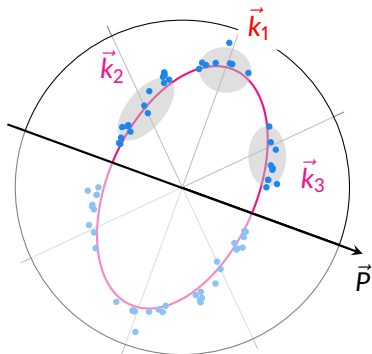


... and in reciprocal space

Resonant X-ray scattering

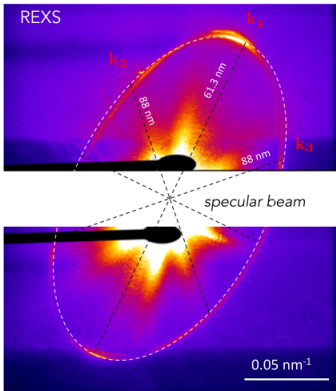


Polar plot of $\frac{2\pi}{\lambda}$ vs \vec{k} direction

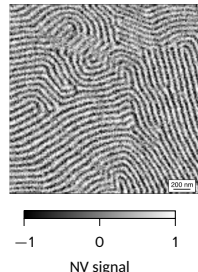
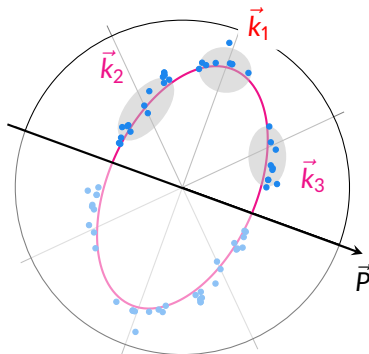


... and in reciprocal space

Resonant X-ray scattering

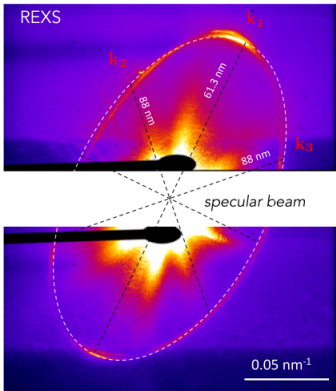


Polar plot of $\frac{2\pi}{\lambda}$ vs \vec{k} direction

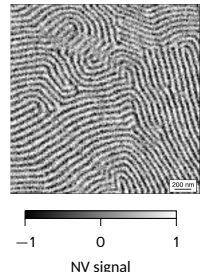
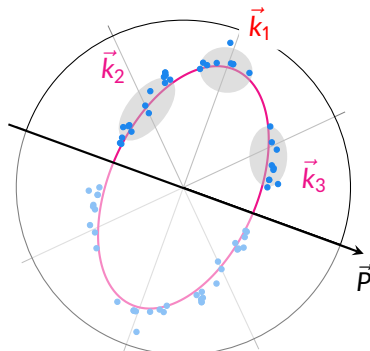


... and in reciprocal space

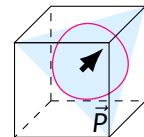
Resonant X-ray scattering



Polar plot of $\frac{2\pi}{\lambda}$ vs \vec{k} direction



NV signal



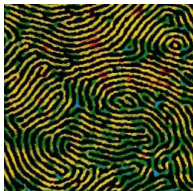
Surface effect? Only \vec{k}_1 seen by neutrons

D. Lebeugle et al. *Phys. Rev. Lett.* 100 (2008), 227602

Universal patterns in lamellar systems

Block copolymer

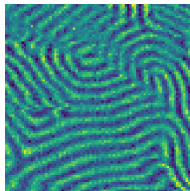
Period 40 nm



 T. A. Witten. *Phys. Today* 43 (1990), 21

BiFeO₃ magnetic cycloid

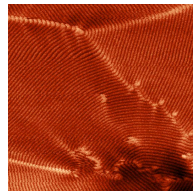
Period 64 nm



 A. Finco et al. *Phys. Rev. Lett.* 128 (2022), 187201

FeGe magnetic helix

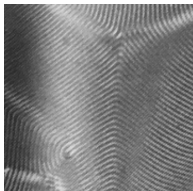
Period 70 nm



 P. Schönherr et al. *Nat. Phys.* 14 (2018), 465

Liquid crystals

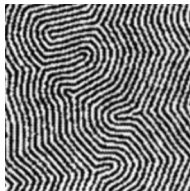
Period 800 nm



 Y. Bouligand. *Dislocations in solids* (1983), Chap. 23

Ferrimagnetic garnet

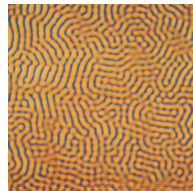
Period 8 μm



 M. Seul et al. *Phys. Rev. A* 46 (1992), 7519

Fluid diffusion

Period 250 μm



 Q. Ouyang et al. *Chaos* 1 (1991), 411

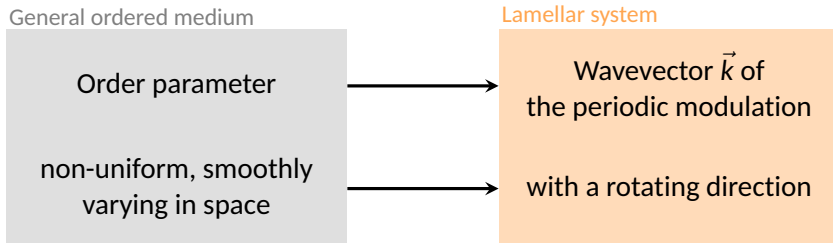
Topological defects in lamellar systems

General ordered medium

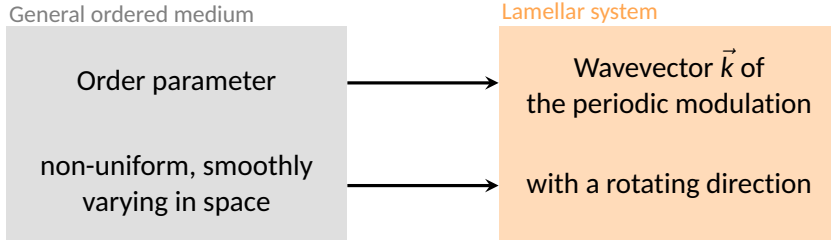
Order parameter

non-uniform, smoothly
varying in space

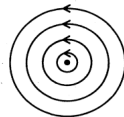
Topological defects in lamellar systems



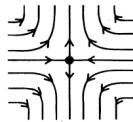
Topological defects in lamellar systems



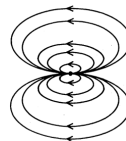
except at singular regions of lower dimensionality → topological defects



disclination
winding number = 1

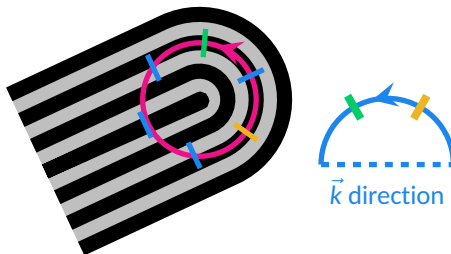
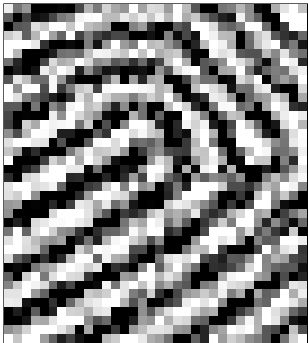


disclination
winding number = -1



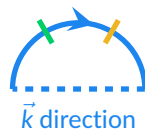
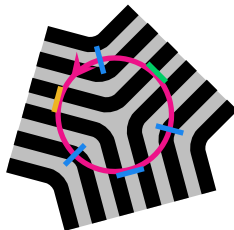
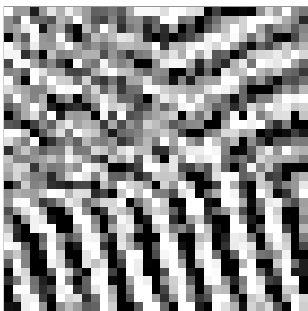
disclination
winding number = 2

$+\pi$ -disclination



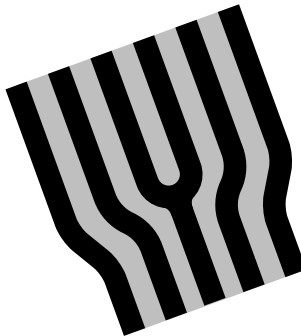
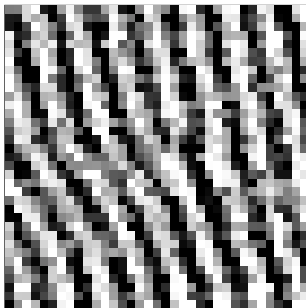
winding number $+1/2$

$-\pi$ -disclination



winding number $-1/2$

Edge dislocation

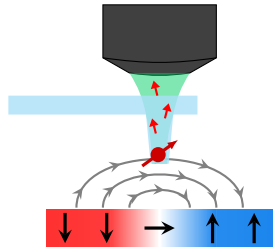


Combination of
 $+\pi$ - and $-\pi$ -disclinations

winding number 0

Summary

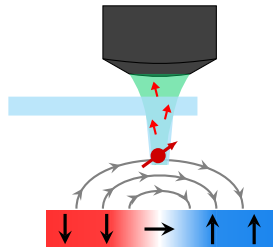
NV center magnetometry



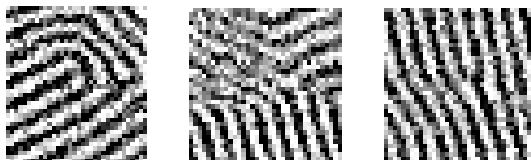
- highly sensitive
- nanoscale
- quantitative
- non-perturbative

Summary

NV center magnetometry



Topological defects in multiferroic BiFeO₃



- highly sensitive
- nanoscale
- quantitative
- non-perturbative

Towards electric control?

A. Finco et al. *Phys. Rev. Lett.* 128 (2022), 187201

Acknowledgments

L2C, Montpellier

Angela Haykal, Pawan Kumar, Vincent Jacques

UMR CNRS/Thales, Palaiseau

Pauline Dufour, Vincent Garcia, Stéphane Fusil

SPEC, CEA Gif-sur-Yvette

Anne Forget, Dorothée Colson, Jean-Yves Chauleau, Michel Viret

Synchrotron Soleil

Nicolas Jaouen



European Research Council
Established by the European Commission

